A Multimode High-Frequency Inductor Model

A new inductor model accurately characterizes high frequency behavior through multiple resonances

By Randall W. Rhea
Eagleware Corporation

It is shown that the classic inductor model poorly predicts inductor behavior at high frequencies. This article begins with a review of that classic model, and the roots of its failure are pondered. A simple model is then proposed which is valid through multiple-resonant modes. The multimode model is then applied to a variety of inductor types to demonstrate its accuracy. In just one case — short inductors with tight coupling between input and output windings — does the multimode model require additional refinement.

The classic model

The objective of this paper is not to formulate the low frequency (static) inductance of the inductor but to advance a new model valid for predicting high-frequency behavior. However, a review of static inductance and the classic model is helpful. The classic inductor model is given in Figure 1. Inductance is given by:

$$L = \frac{\mu_0 n^2 \pi a^2}{c} \times K \text{ henries} \qquad (1)$$

where K is dependent only on the shape of the coil.

Wheeler [1] presented an expression for K which for a current sheet is essentially exact:

$$K = \frac{1}{3\pi}\left\{\frac{dc}{a^2}\left[F(k) - E(k)\right] + \frac{4dE(k)}{c} - \frac{8a}{c}\right\} \qquad (2)$$

where a = mean radius of the solenoid; c = axial length of the solenoid; $d = \sqrt{4a^2+c^2}$; n = number of turns; $k = 2a/d$; $F(k)$ = complete elliptic integral of the first kind; and $E(k)$ = complete elliptic integral of the second kind. (All units are MKS.)

Wheeler also provided approximations of his formula which do not involve elliptic integrals. Millar [2] provided a procedure for evaluating the elliptic integrals, and Lundin [3] provided formulas believed more accurate than those of Wheeler. Pursuit of additional precision is probably unjustified, since these formula assume a current sheet which only approximates physical solenoids with round wire. Solenoids with round wire were addressed by the National Bureau of Standards [4] and Klappenberger [5].

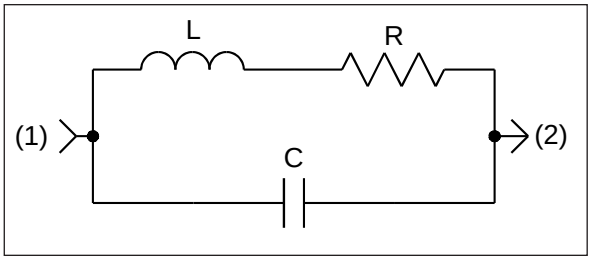

■ **Figure 1. Schematic diagram of the classic inductor model.**

The inductance is simply found with a stated accuracy of about 1 percent using Wheeler's earlier and well known formula:

$$L = \frac{n^2 a^2}{9a + 10c} \text{ microhenries} \qquad (3)$$

where the unit of length is inches. The accuracy of this formula is overstated for real wire diameters because the current migrates inward at higher frequencies, making the effective solenoid radius less than the mean radius. Because we are concerned with high-frequency inductor behavior, we will use the inside radius when computing inductance.

The concept of parasitic capacitance in the inductor is a century old [6, 7, 8]. Hubbard [9] found the capacity of the single-layer solenoid inductor, with one end grounded, as a function

of the solenoid shape and size. Butterworth [10] expended considerable mathematical effort toward finding the resistance of the solenoid, unfortunately with questionable results. This author is unaware of any worker who mathematically attacked either the resistance or capacitance problem and was rewarded for doing so. This is an important point which will be revisited.

Medhurst [11] abandoned mathematical approaches and empirically found useful formulations for both solenoid resistance and capacitance. Medhurst is recommended reading for those interested in the inductor.

The capacitance due to Medhurst is:

$$C = H \times D \qquad \text{picofarads} \qquad (4)$$

where $D = 2a$ and H is only a function of the length to diameter ratio, $c/2a$. The unit of length is centimeters. The value of H versus $c/2a$ is given in Table 1.

The fact that capacitance is not a function of the solenoid wire spacing is certainly not intuitive. This is another interesting point later clarified by the proposed model.

The resistance due to Medhurst [11] is found from the unloaded Q, Q_u:

$$Q_u = 0.15a\psi\sqrt{f_0} \qquad (5)$$

where the unit of length is centimeters; f_0 is the frequency in hertz; and ψ is a function of $c/2a$ and the spacing ratio. The spacing ratio, d_w/s, is the fraction of c occupied by wire. Values of ψ versus $c/2a$ and d_w/s are given in Table 2.

Experimental verification of the classic model

Vertically-mounted solenoid.

Shown in Figure 2 is a single-layer 18 gauge copper wire solenoid mounted vertical to an aluminum 2 by 3 inch ground plate. The solenoid is soldered to a small brass shim with gravity contact to the plate. SMA connectors separated by 1 inch are threaded into the plate. Shims of 0.2 by 0.3 inch are soldered to the SMA center pins to capacitively couple to the solenoid. The solenoid is 12.9 turns with a mean radius of 0.268 inches and a mean length of 0.89 inches. The first turn is approximately 0.125 inches above the plate via a short right-angle bend in the wire.

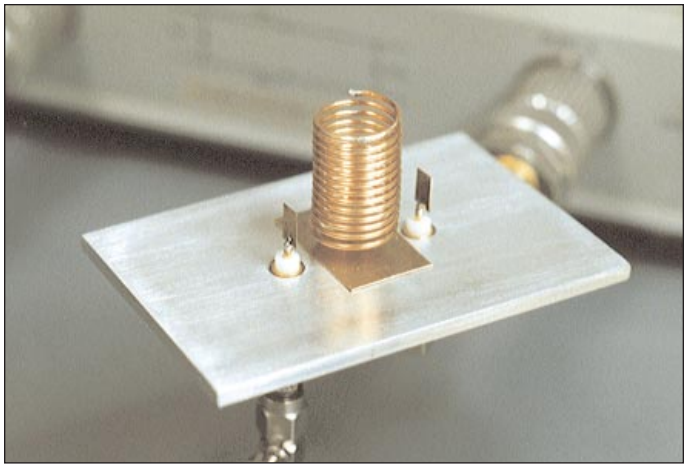

■ **Figure 2. Vertically mounted solenoid in a transmission text fixture with capacitance coupling to the solenoid.**

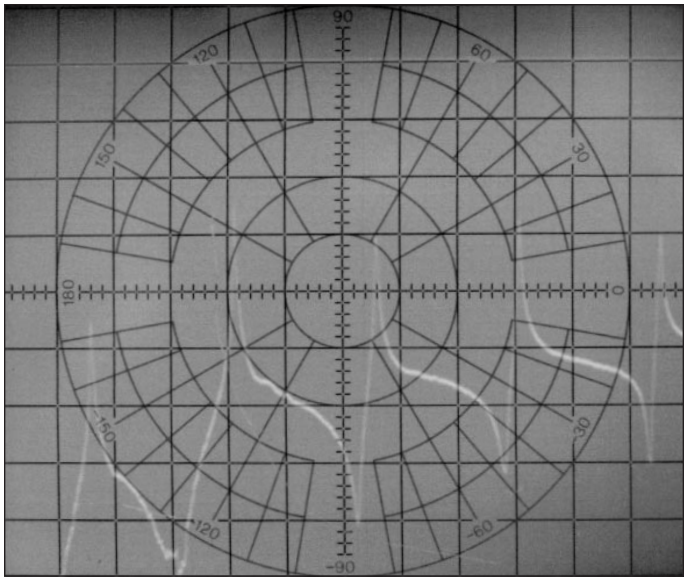

■ **Figure 3. Transmission amplitude response of the vertically mounted solenoid in Figure 2. The sweep range is 500 kHz to 1300 MHz (approximately 108 MHz/DIV).**

c/2a	H	c/2a	H	c/2a	H
50	5.8	5.0	0.81	0.70	0.47
40	4.6	4.5	0.77	0.60	0.48
30	3.4	4.0	0.72	0.50	0.50
25	2.9	3.5	0.67	0.45	0.52
20	2.36	3.0	0.61	0.40	0.54
15	1.86	2.5	0.56	0.35	0.57
10	1.32	2.0	0.50	0.30	0.60
9.0	1.22	1.5	0.47	0.25	0.64
8.0	1.12	1.0	0.46	0.20	0.70
7.0	1.01	0.90	0.46	0.15	0.79
6.0	0.92	0.80	0.46	0.10	0.96

■ **Table 1. Capacitance factor *H*, as a function of solenoid *c/2a* ratio.**

	c/2a							
d_w/s	0.2	0.4	0.8	1.0	2	4	8	∞
1.0	0.18	0.26	0.35	0.38	0.63	0.80	0.93	0.92
0.9	0.24	0.33	0.43	0.47	0.69	0.84	0.93	0.91
0.8	0.28	0.40	0.50	0.55	0.75	0.87	0.91	0.89
0.7	0.32	0.46	0.58	0.61	0.78	0.87	0.89	0.87
0.6	0.34	0.49	0.63	0.67	0.78	0.85	0.86	0.85
0.5	0.34	0.48	0.61	0.65	0.74	0.80	0.82	0.81
0.4	0.31	0.45	0.56	0.60	0.69	0.74	0.76	0.76
0.3	0.25	0.37	0.49	0.52	0.60	0.64	0.67	0.68
0.2	0.19	0.27	0.36	0.39	0.45	0.49	0.51	0.53
0.1	0.10	0.14	0.19	0.21	0.25	0.27	0.29	0.30

■ **Table 2. Values of ψ versus *c/2a* and d_w/s.**

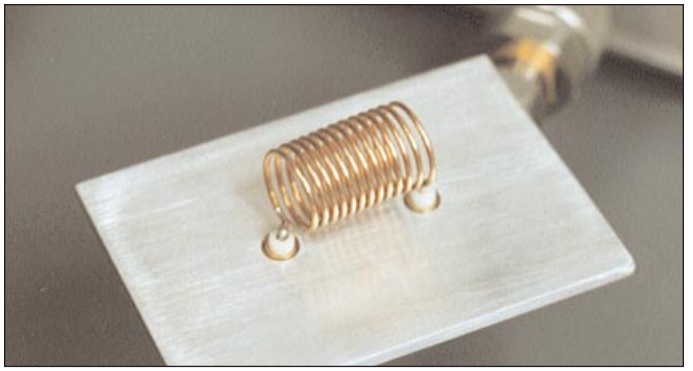

■ **Figure 4. Horizontally mounted solenoid in the transmission test fixture.**

The inductance using Equation (3) is 916 nH, using an inside solenoid radius of 0.248 inches. The capacitance due to Medhurst is 0.69 pF using the mean radius. The resonant frequency of this capacitance with 916 nH is 200 MHz.

Shown in Figure 3 is the swept forward magnitude and phase S-parameter response from 0.5 to 1300 MHz measured using an HP8505A network analyzer with an HP8503A S-parameter test set. The first resonance measured with markers is approximately 189 MHz.

Solenoid mounted parallel to a ground plate.

The solenoid was next mounted parallel to the ground plate. This provides a means of direct coupling to the solenoid and is consistent with common PWB mounting methods used today. Figure 4 is a photograph of this configuration. The outer radius of the solenoid is approximately 0.135 inches above the plate. The analyzer was calibrated back to back using an SMA double-female connector with a phase length similar to the two SMA connectors mounted to the plate. The swept response is given in Figure 5.

The new multimode model

Given in Figure 6 is the response of the classic inductor model in Figure 1 for the solenoid shown in Figure 4.

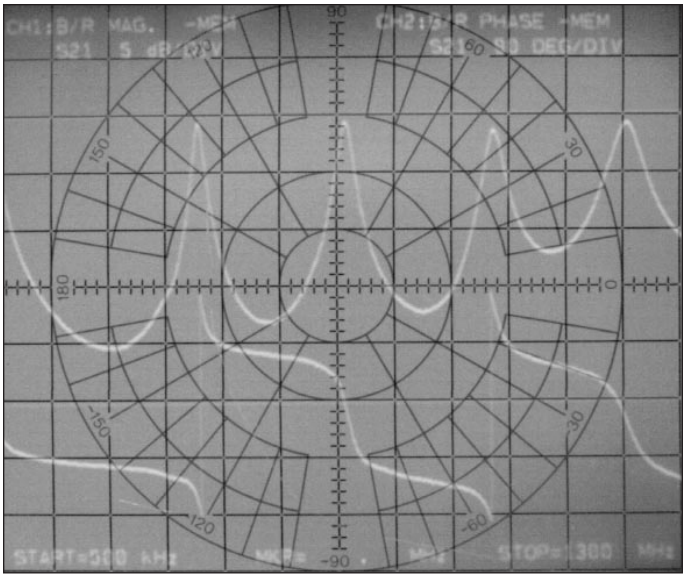

■ **Figure 5. Transmission amplitude and phase response of the horizontally mounted solenoid.**

The slope of the magnitude responses at low frequency, which is a measure of static inductance, is similar for the classic model and the measured data. The first anti-resonant modes (transmission minima) occur at similar frequencies for the classic model and the measured data. *Despite these similarities, it is clear that the classic model totally fails to predict the high-frequency behavior of the solenoid.* The multiple resonant modes which are evident in the magnitude response in Figure 5 are not present in the classic model, and the transmission phase at the first anti-resonance is incorrect.

A simple lumped model cannot predict the multiple resonances present in the measured data. While a lumped model with multiple elements could model this behavior, the periodic nature of the measured data in Figure 5 strongly suggests a transmission line model. The response in Figure 7 of a one-element series transmission line model fits the measured data extremely well and suggests the inductor is in reality a transmis-

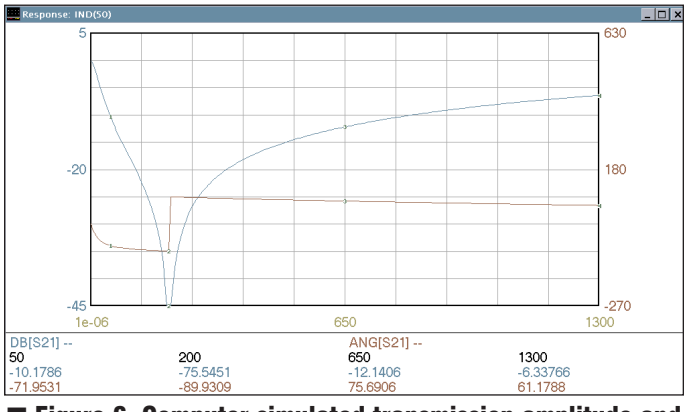

■ **Figure 6. Computer simulated transmission amplitude and phase response of the classic model of the solenoid shown in Figure 4.**

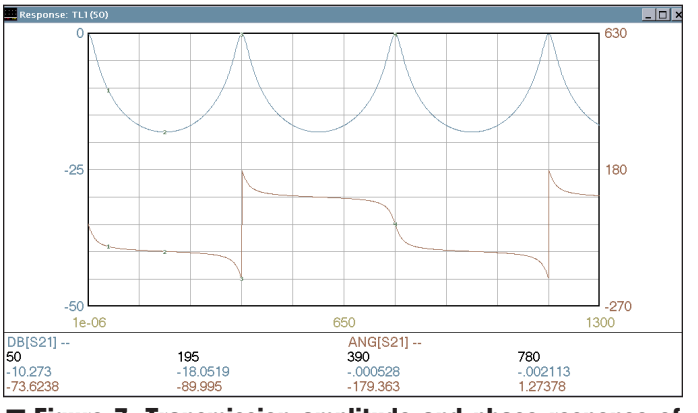

■ **Figure 7. Transmission amplitude and phase response of the simple proposed transmission line model for inductor. Transmission line impedance and length are adjusted to match the measured response.**

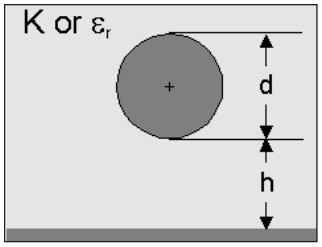

■ **Figure 8. Diagram of the wire over ground transmission line.**

sion line. When the transmission line parameters are adjusted to fit the measured data, the characteristic impedance Z_0 is 796 Ω and the electrical length θ is 600 degrees at 1300 MHz. These parameters were selected to fit the frequency of the first resonance and the depth of the first two anti-resonant modes. Model refinement with additional capacitors to better fit the secondary effects of the response is discussed later.

The elegance of this model is further secured when it is shown that the distributed parameters of the transmission line relate directly to the low frequency inductance and the capacitance to ground of the solenoid!

In fact, the required transmission line parameters are related to the low frequency inductance, L_0, and capacitance, C_0, by the classic formula:

$$Z_0 = \sqrt{\frac{L_0}{C_0}} \text{ ohms} \qquad \text{and,} \qquad (6)$$

$$\theta = 2\pi f_0 \sqrt{L_0 C_0} \text{ radians} \qquad \text{or,} \qquad (7)$$

$$\theta = 360 f_0 \sqrt{L_0 C_0} \text{ degrees} \qquad (8)$$

Parameter extraction

Static data — The in-fixture inductance of the solenoid in Figure 4 measured with a digital *L-C* meter is 986 nH after deembedding of the estimated inductance of the SMA connectors. The measured capacitance to ground of the solenoid is 1.73 pF after deembedding. The accuracy of the meter is not tracable but is estimated to be within 1 percent. That the inductance measured by the *L-C* meter is higher is not unexpected, considering the effective solenoid radius is higher at low frequencies. The transmission line parameters of the solenoid from the measured static inductance and capacitance and Equations (6) and (8) are Z_0 = 728 Ω and θ = 590 degrees at 1300 MHz, in reasonable agreement with the values that fit the model to the measured data.

Fit to data — A second method for extracting transmission line parameters for the model is to iterate Z_0 and θ of the line to fit measured data for the solenoid. An advantage of this method is that the solenoid is modeled "in-circuit," or in the actual environment of the solenoid. This significantly relaxes the deembedding effort and improves accuracy.

Approximate methods

It is shown next that the transmission line parameters may be found from the static inductance using one of the standard formulas and the static capacitance using numerous approximate formulas for the capacity of transmission lines. The solenoid is replaced with a solid cylinder for the capacitance calculation.

Solenoid parallel to ground.

Consider the solenoid in Figure 4. Again, L_0 computed from Equation (3) is 916 nH using the inside radius. C_0 will be computed using formulas for the characteristic impedance of a wire over ground as in Figure 8. In this case, the "wire" is the solenoid acting as a cylinder. The characteristic impedance of this cylinder over ground [12] is

$$Z_c = \frac{59.952}{\sqrt{\varepsilon_r}} \ln\left[\left(1+\frac{2h}{d_c}\right)+2\sqrt{\frac{h}{d_c}\left(1+\frac{h}{d_c}\right)}\right] \text{ ohms} \qquad (9)$$

where h = height above ground of the cylinder edge; d_c = cylinder outer diameter; and ε_r = relative dielectric constant of surrounding media.

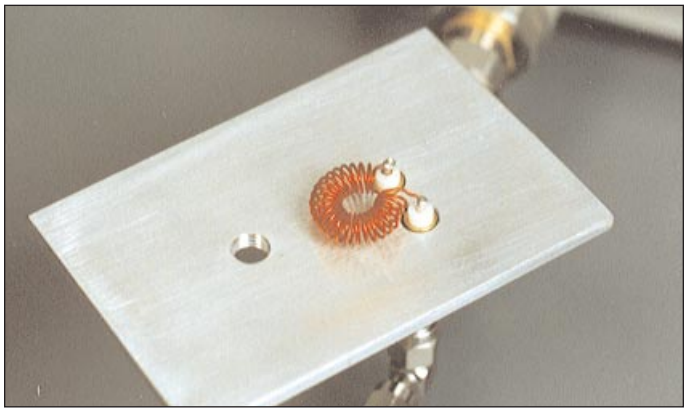

■ **Figure 9. Toroid inductor mounted in the transmission test fixture.**

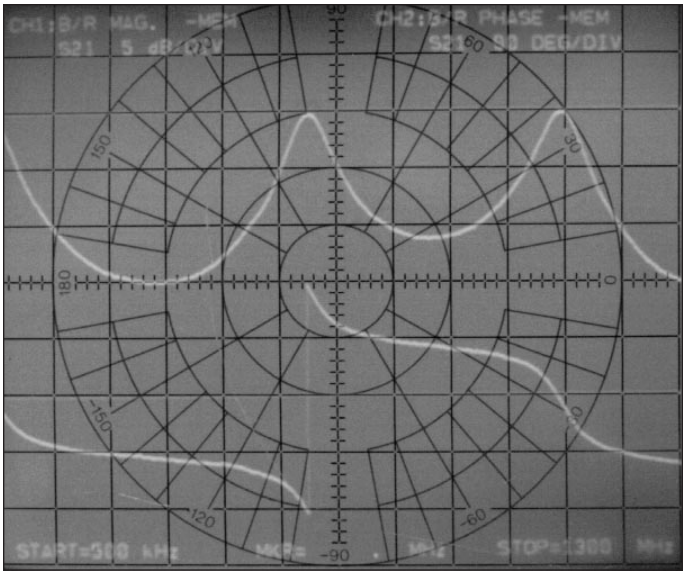

■ **Figure 10. Transmission amplitude and phase response of the toroid inductor.**

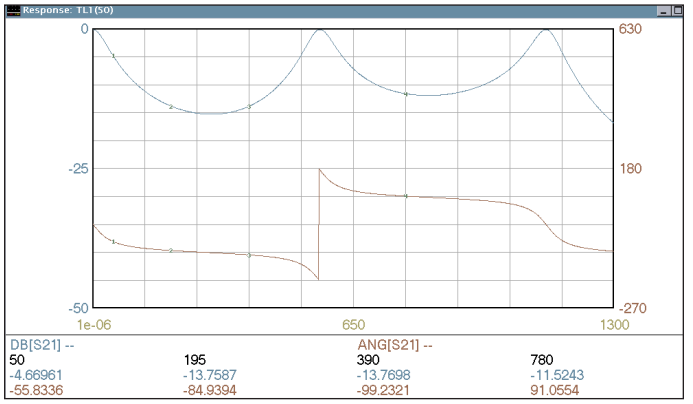

■ **Figure 11. Computer simulated transmission amplitude and phase responses of the transmission line model of the toroi plus 0.12 pF of parallel capacitance.**

The capacitance is then found from the characteristic impedance of the cylinder:

$$C_0 = c\frac{\sqrt{\varepsilon_r}}{V_0 Z_c} \text{ farads} \qquad (10)$$

where V_0 is the velocity of light in a vacuum.

C_0 for the solenoid in Figure 4 computed using this technique is 1.34 pF. Z_0 and θ for the transmission line model computed from these L_0 and C_0 are 827 Ω and 518 degrees at 1300 MHz, respectively.

Toroid parallel to ground.

The static inductance of a toroid [13] is approximately

$$L_0 = 11.7\mu_r tn^2 \log\left(\frac{OD}{ID}\right) \text{ nanohenries} \qquad (11)$$

where OD = the mean outer diameter of the winding; ID=the mean inner diameter of the winding; t = (OD – ID)/2; and μ_r = the relative permeability of the core.

This formula assumes tight flux linkage and a winding which occupies the full circumference of the core.

Shown in Figure 9 is a toroid inductor with 26 turns of 0.020 inch diameter wire on a 300 degree arc of air core, OD = 0.58 and ID = 0.22, mounted 0.050 inches above ground. L_0 computed from (11) is 599 nH, and C_0 computed using the wire over ground procedure and an effective cylinder length of 1.05 inches is 1.62 pF. The measured static L_0 is 450 nH and C_0 is 1.74 pF. The significant error of the toroid formula explains why inductance is often computed using the inductance index, A_L, which condenses all factors in Equation (11) except n^2 into a single empirically found index. From the measured data on this toroid, we find A_L = 0.666 nanohenries per turn squared.

The toroid places the input and output terminals of the inductor in closer proximity. This introduces capacitance in parallel with the inductor.

The measured response of this toroid is given in Figure 10. Given in Figure 11 is the response of the transmission line model with L_0 = 450 nH and C_0 = 1.74 pF (Z_0 = 509 Ω and θ = 414 degrees at 1300 MHz). In addition, a capacitance of 0.12 pF is placed in parallel with the model, terminal to terminal. This parallel capacitance is responsible for increased attenuation for the first and higher odd-order anti-resonant modes and reduced attenuation and even-ordered anti-resonant modes as seen in Figure 11. We will return to this subject.

Solenoid parallel to ground with dielectric

The wire over ground procedure can be extended to solenoids mounted over a ground with a substrate material separating the ground and solenoid. Shown in Figure 12 are a pair of Coilcraft 132 series solenoids. A 132-20SM coil with 20 turns was mounted over ground with an FR4 dielectric 0.060 inch thick spacer. The inductance calculated from measured dimensions and

■ **Figure 12. Coilcraft 132 surface mount series of solenoid inductors.**

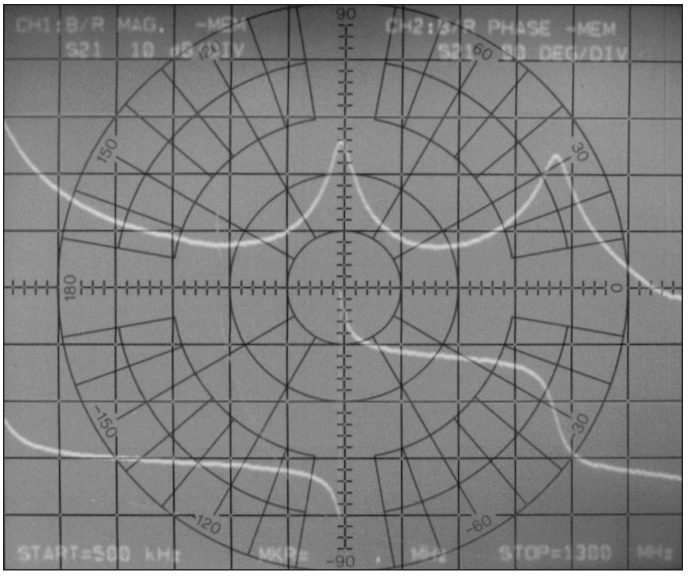

■ **Figure 13. Transmission amplitude and phase response of the Coilcraft 132-20SM mounted on an FR4 substrate.**

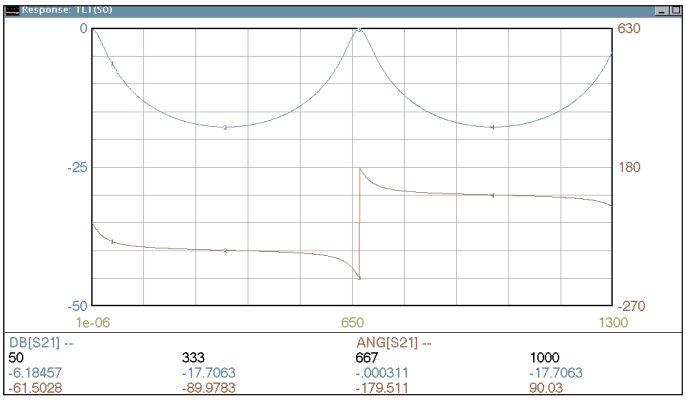

■ **Figure 14. Computer simulated amplitude and phase response of the proposed transmission line model of the Coilcraft 132-20SM mounted over FR-4 substrate.**

Equation (3) using the inside radius is 573 nH. The inductance specified by Coilcraft is 558 nH. C_0 computed using the round microstrip formula by Gunston [12] with an FR4 substrate and $\varepsilon_r = 4.8$ is 0.98 pF. The measured static inductance and capacitance are 589 nH and 0.95 pF. Figure 13 is the measured response and Figure 14 is the transmission line model response using the computed inductance and capacitance ($Z_0 = 765\ \Omega$ and $\theta = 351$ degrees).

Helical coax

The transmission line model parameters for helical coax are found from L_0 using Equation (3) with a correction factor for shielding, and from C_0 as a coaxial capacitor assuming the solenoid is a cylinder. Again the results are encouraging.

Shown in Figure 15 is a solenoid and its coaxial shield. The solenoid is 16 turns of 0.04 inch diameter wire with an inside radius of 0.072 and length of 1 inch. The inductance without a shield computed from

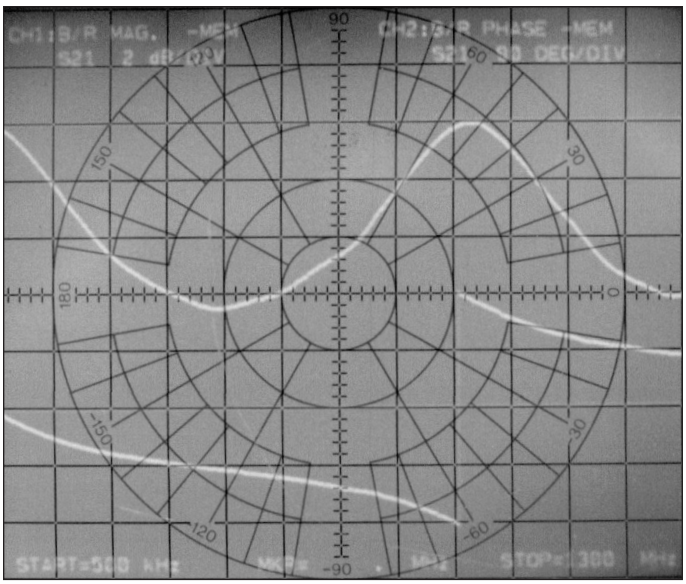

■ **Figure 16. Measured transmission amplitude and phase response of the coaxial helical solenoid.**

■ **Figure 15. The coaxial helical solenoid, removed from its shield.**

Equation (3) is 125 nH.

A formula for the effect of a conducting, non-magnetic, shield on inductance was given by Bogle [14]:

$$LF = 1 - \frac{\left(\frac{a}{a_s}\right)^2}{1 + \frac{1.55(a_s - a)}{c}} \qquad (12)$$

where a_s=the radius of the shield.

The results are similar to the nomographs in [15]. If the solenoid radius is much smaller than the shield diameter, the inductance correction factor approaches 1. The inside diameter of the shield in Figure 15 is 0.350 inches and the inductance reduction factor using the solenoid inside radius is 0.970. The resulting inductance found by multiplying the results of Equation (3) by Equation (12) is 121 nH. The measured static inductance of the shielded solenoid is 121 nH.

The static coaxial capacitance is found from Equation 10 with a characteristic impedance of 26.77 Ω, resulting from a coaxial inner diameter of 0.224 inches and an outer diameter of 0.350. C_0 found by this procedure is 3.17 pF. The measured static capacitance is 3.07 pF.

The measured response of the helical inductor is given in Figure 16 and the response using $Z_0 = 184\ \Omega$

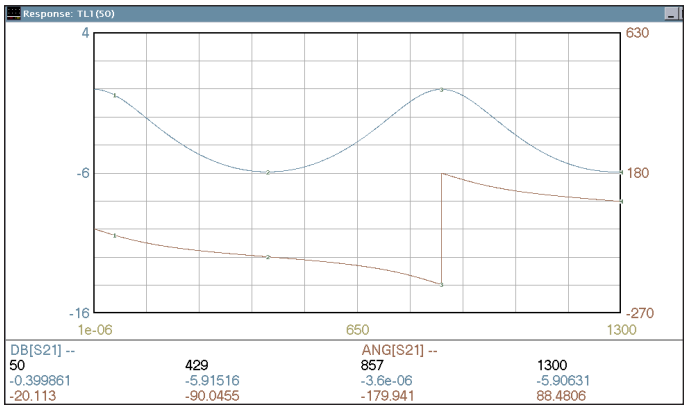

■ **Figure 17. Computer simulated transmission amplitude and phase response of the transmission line model of the coaxial helical solenoid.**

and θ = 273 degrees for the transmission line model from the computed L_0 and C_0 is given in Figure 17.

Additional remarks

Earlier it was stated that mathematical attempts to find solenoid capacitance have been unsuccessful, and next we speculate why this is so.

Medhurst [11] defines the total sum of capacitance between turns as effective parallel "internal" capacitance and the total sum of capacitance between turns and ground as effective parallel "external" capacitance. The total parallel capacitance in the classic model is the sum of the internal and external capacitance. However, how can we justify considering capacitance to ground as capacitance in parallel with the solenoid? This paper demonstrates that excellent agreement with measured data is achieved when it is assumed that the distributed solenoid capacitance is referenced to ground, not in parallel with the solenoid. It then follows that the distributed series inductance and distributed capacitance to ground of the solenoid are indistinguishable from the distributed model of a transmission line.

However, the inter-winding internal capacitance can be intuitively viewed as being in parallel with the solenoid. Why, then, is parallel capacitance relatively unimportant in predicting the behavior of the inductor examples above? When the solenoid is long ($c>a$) and there are many turns, the phase shift of an exciting signal between turns is small. The small potential difference between turns therefore results in little capacitive coupling between turns. The phase difference is more significant between non-adjacent turns, but their increased physical spacing results in less capacitance. *Consequently, internal capacitance is a secondary aspect of the solenoid and a mathematical effort to find solenoid capacitance based on the inter-winding capacitance is doomed.*

The phase difference between turns increases as the solenoid radius is increased, the length is decreased and the number of turns are reduced. In this case, the potential difference between turns is significant and the transmission line model requires parallel capacitance.

■ **Figure 18. Solenoid with extreme diameter to length ratio, mounted in the tranmission test fixture.**

Shown in Figure 18 is a solenoid with extreme radius to length. It consists of four turns of 0.020 inch diameter wire with a mean solenoid radius of 0.645 and a length of 0.08 inches. The measured static inductance and capacitance is 1046 nH and 1.17 pF. The measured response is shown in Figure 19.

Given in Figure 20 is the schematic of a transmission line model with added parallel capacitance. It was necessary to divide the transmission line into multiple segments, presumably so capacitive coupling is included between turns with different phase shifts. The model parameters are adjusted to fit the measured data and the resulting response is given in Figure 21.

These additional capacitive elements may also be used to improve agreement between the model and measured data. Non-harmonic periods and unequal attenuation depths of anti-resonant modes are two errors of the simple model which are corrected by these additional elements. There is little need to use inductors at higher-order modes and this additional complexity is typically unjustified because the behavior of inductors at frequencies above the first resonant mode affect only circuit stopbands.

Computer model

A solenoid inductor model for use with the Eagleware GENESYS circuit simulator =SuperStar= Professional is available at the Founder's Forum on the company's web site, www.eagleware.com. This multimode transmission line model uses Equation (3) for the static inductance and the wire over ground procedure, with or without a dielectric substrate, for the static capacitance. The unloaded Q is due to Medhurst and is therefore only valid well below the frequency of the first anti-resonance mode. A desirable follow-up to this article would be to extend this theory to model the unloaded Q of the inductor at least through the frequency of the first resonance.

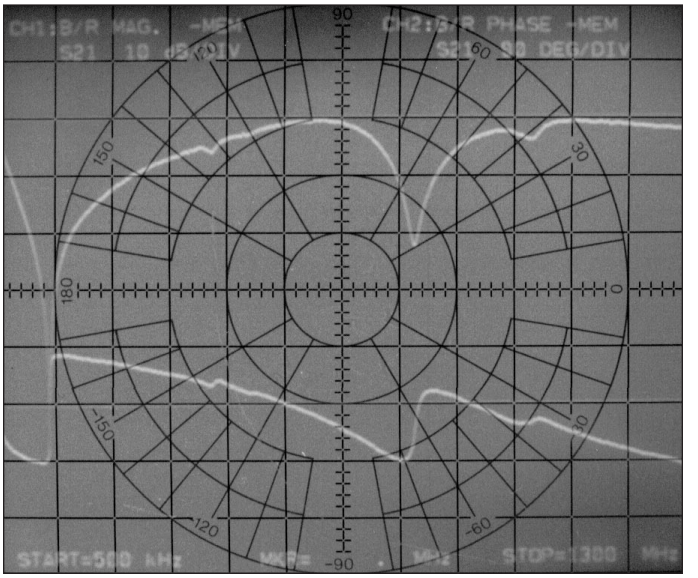

■ **Figure 19. Measured transmission amplitude and phase response of the extreme diameter to length ratio solenoid.**

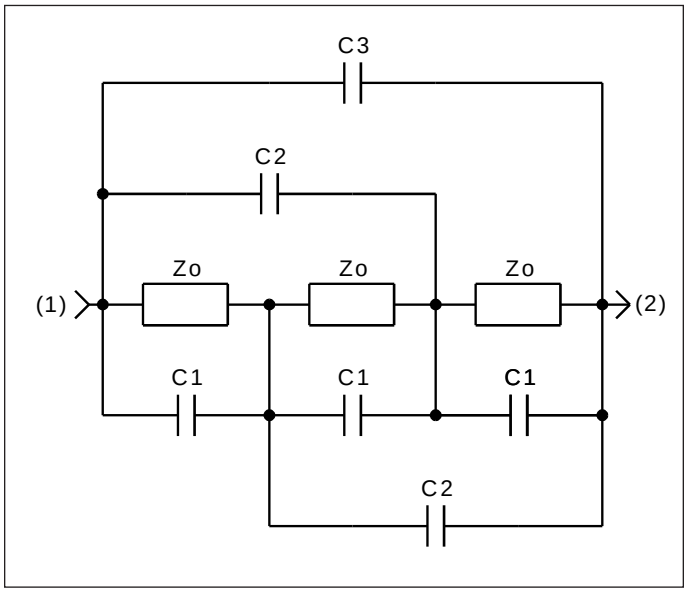

■ **Figure 20. Transmission line solenoid model, including interwinding capacitance typically required for solenoids with extreme diameter to length ratios.**

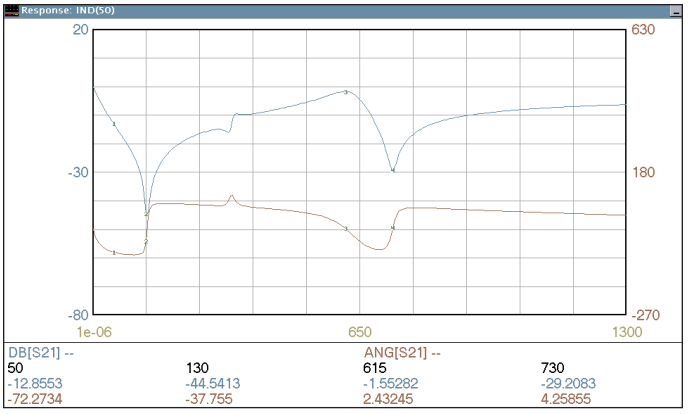

■ **Figure 21. Computer simulated transmission amplitude and phase responses of the model in Figure 20.**

Summary

A new model for the high-frequency behavior of inductors is presented. Evidence suggests that the inductor is in reality a transmission line. That this is so is further suggested by the simplicity of the transmission line model which predicts behavior through multiple resonant modes and for which the distributed inductance and capacitance of the model relate intuitively and easily to physical parameters. The classic model is highly suspect and it is speculated its erroneous development was based on a test procedure which detects only the first anti-resonant mode. Coincidentally, this resonance is similar in lumped and distributed models.

These summarizing remarks are most evident in long or shielded coils. The case for the transmission line model is weakest in coils well removed from ground with small length to radius ratios. It is conceivable that two distinctly different operational modes exist for inductors, one for long inductors with weak capacitive coupling between turns and one for short dense-winding inductors with strong capacitive coupling. ■

References

1. H. A. Wheeler, "Inductance Formulas for Circular and Square Coils," *Proc. IEEE*, Vol. 70, pp 1449-1450, 1982.

2. H. C. Millar, "Inductance Formula for a Single-Layer Circular Coil," *Proc. IEEE*, Vol. 75, No. 2, pp 256-257, 1987.

3. R. Lundin, "A Handbook Formula for the Inductance of a Single-Layer Circular Coil," *Proc. IEEE*, Vol. 73, pp 1428-1429, September 1985.

4. *Radio Instruments and Measurements*, Circular of the National Bureau of Standards C74, March 10, 1924, corrected January 1, 1937.

5. A. Klappenberger, "Designing Accurate Small Inductors for Microwave L-C Filters," *RF Design*, pp 52, 55, November 1994.

6. A. G. Webster, "An Experimental Determination of the Period of Electrical Oscillations," *Physical Review*, Vol. VI, pp 297-314, 1898.

7. P. Drude, *Ann. d. Physics (4)*, 9, 1902

8. W. Lenz, *Ann d. Physics (4)*, 43, 1914

9. J. C. Hubbard, "On the Effect of Distributed Capacity in Single Layer Solenoids," *Physical Review*, Vol. 9, pp 529-541, 1917.

10. S. Butterworth, "Effective Resistance of Inductance Coils at Radio Frequencies," *Exp. Wireless and Wireless Engineer*, Vol. 3, pp 203, 302, 417 and 483, 1926.

11. R. G. Medhurst, "H.F. Resistance and Self-Capacitance of Single-Layer Solenoids," *Wireless Engineer*, pp 35-43, February 1947, and pp 80-92, March 1947.

12. M. A. R. Gunston, *Microwave Transmission-Line Impedance Data*, Noble Publishing, 1996.

13. R. W. Rhea, *HF Filter Design and Computer Simulation*, Noble Publishing, 1994.

14. A. G. Bogle, "The Effective Inductance and Resistance of Screened Coils," *Jour. IEE*, p 299, 1940

15. Howard W. Sams, *Reference Data for Engineers: Radio, Electronics, Computer, and Communications*, 7th ed., 1986.

Author information

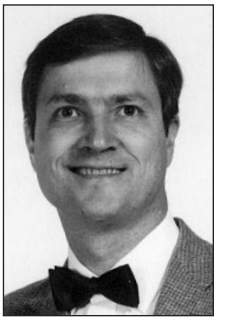

Randall W. Rhea is founder and principal owner of Eagleware Corporation, 1750 Mountain Glen, Stone Mountain, GA 30087, a leading supplier of RF/microwave design software. He holds a BSEE from the University of Illinois and an MSE from Arizona State University and is the author of numerous books, book sections and technical articles. He may be reached by fax at (770) 939-0157 or by e-mail at eagleware@eagleware.com.